सीएसआईआर- एम्प्री
CSIR-AMPRI

Effect of Temperature on Optical Energy Band Gap of $BaTiO_3$ Nanoparticles

Hariom Pawar[a,b*], U. K. Dwivedi[b], Tara Prasad[b] and Deepshikha Rathore[b*]

[a]*JECRC University, Jaipur 303905 (Rajasthan), India*
[b]*Amity University Rajasthan, Jaipur 303002 (Rajasthan), India*

Abstract : The purpose of this research is to investigate connection between optical energy band gap and calcination temperature with including dielectric properties. BaTiO3 nanoparticles were prepared by Sol-Gel route atLTH by changing calcination temperature. The physicochemical properties like structural, optical, and dielectric properties were studied by XRD, UV-VIS spectroscopy, DFT, and LCR meter. Synthesized BaTiO3 nanoparticles gained amorphous to cubic crystalline phase with varying calcination temperature which were confirmed using XRD analysis. The optical energy band structure and shifting of absorbance edge towards lower wavelength respecting change in time and calcination temperature were examined using density functional theory (DFT) and UV-VIS spectroscopy, respectively. The dielectric properties of BaTiO3 nanoparticles were examined with varying temperature from 30 ℃ to 170 ℃.

Keywords: Density functional theory (DFT);cubic phase; nanoparticles; optical energy band gap.

Introduction

BaTiO3 is a very prominent ferroelectric material which shows ferroelectric properties even at room temperature, low corrosion proportion, small dielectric loss, and high dielectric constant. The BaTiO3 in nanoscale unveils improved novel magnetic, optical, electronic, mechanical, and chemical properties which is difficult to acquire from their bulk nature1-3. The unique properties of synthesized BaTiO3 nanoparticles are cast-off for transducers, memory devices, sensors, multilayer capacitors (MLCs) and fabrication of capacitor4-6. In this paper, BaTiO3 nanoparticles is prepared using Sol-Gel route. The effect of varying time with calcination temperature on optical energy band gap of BaTiO3 nanoparticles is examined, including investigation of low energy loss with enhanced dielectric constant, that is not conveyed in literature up to now.

Experimental Details

BaTiO3 nanoparticles were prepared using Sol-Gel route. Deionized water, Barium acetate (Sigma-Aldrich), Titanium tetra-iso-propyl alkoxides (TTIP) (Sigma-Aldrich), 2-Propanol (Qualigens), and Acidic acid Glacial (SRL) were selected in 150:1:1:1:6 molar ratio, individually. The whole chemical reaction was handled in three phases which is described here in Figure 1.The density functional theory (DFT) was established by the Quantum ESPRESSO software to estimate the energy of cubic BaTiO3 nanoparticles. The optical properties were determined by UV-VIS

spectroscopy (thermos scientific, (Model BIOMATE-3S)). Pellets of synthesized samples were obtained by KBR Hydraulic press which were coated by silver paste to make ohmic contact. The dielectric assets of calcinated BaTiO3 nanoparticles were investigated by LCR meter (HIOKI, IM3536) with varying temperature (30-150) through a frequency range (40-5MHz).

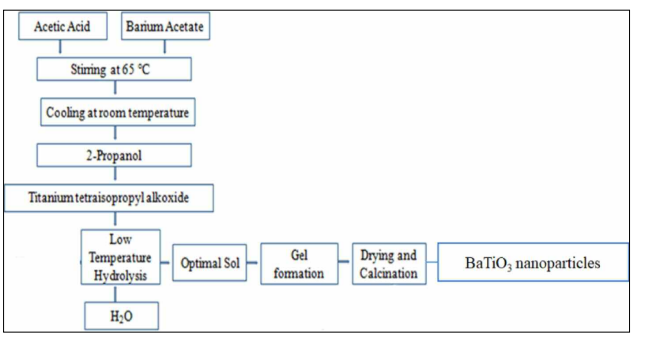

Figure 1. Schematic representation of the synthesis of BaTiO3 nanoparticles.

*Corresponding author:(E-mail: hariomforensic@gmail.com)

Results and Discussion

Structural and Morphological properties

XRD study of $BaTiO_3$ nanoparticles calcinated with varying times and different temperatures was depicted in Figure 2. All samples were prepared using Sol–Gel route. Figure 2 (a) showed amorphous form of $BaTiO_3$ with carbonate impurities that was calcinated at 100 for 1 hour. Moreover, it was also observed from Figure 2 (b–e) that the synthesized $BaTiO_3$ nanoparticles calcinated on 600 for 2 hours besides 5 hours correspondingly, achieved cubic crystal-like phase with less impurity of $BaCO_3$. Furthermore, the $BaTiO_3$ nanoparticles form pure cubic crystalline phase at 800 , which is a like commercially available $BaTiO_3$ (Merck, 99.9%). The peaks of $BaCO_3$ and $BaTiO_3$ were confirmed by JCPDS NO- 40-0373 and JCPDS No-31-0174, respectively. It was confirmed from results that purity of $BaTiO_3$ increases as the calcination temperature rises (100–800 . The morphological properties of synthesized $BaTiO_3$ nanoparticles were reported in previously published article7.

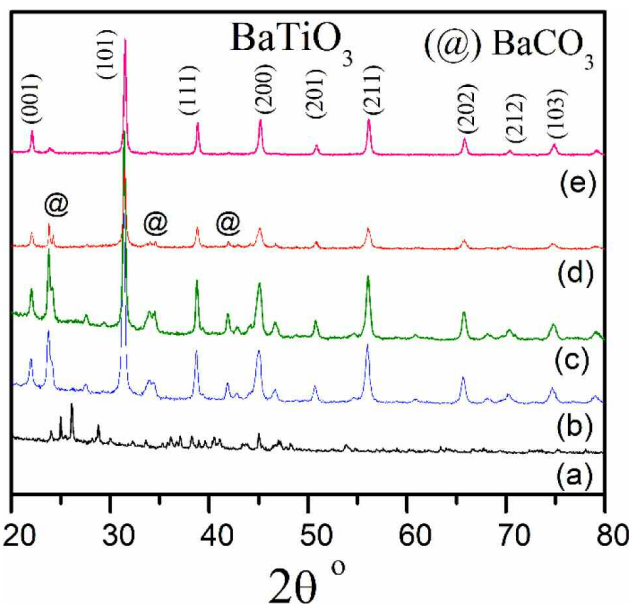

Figure 2. The XRD of $BaTiO_3$ calcinated at (a) 100 , 1 hour, (b) 600 , 2 hours, (c) 600 , 5 hours, (d) 800 , 2 hours and (e) commercially available.

Optical properties

The optical absorbance spectra of $BaTiO_3$ nanoparticles were illustrated in Figure 3. It was observed from Figure 3(I) that the fundamental absorption edge of $BaTiO_3$(a) calcinated at 100 for 1 hour and (b) commercially available found to be nearly 317 nm. The fundamental absorption edges of $BaTiO_3$ nanoparticles, nearly at 383 nm and 370 nm was observed in Figure 3 (II), calcinated at 600 for (a) 2 hours and (b) 5 hours, respectively. Similarly, samples calcinated at (a) 600 and (b) 800 for 2 hours showfundamental absorption edges at 383 nm and 325 nm in Figure 3 (III).

For photon energy E, absorbance is calculated using given formula8,

$$\alpha = \frac{B\,(h\upsilon - E_g)^r}{h\upsilon} \qquad (1)$$

where – absorbance, – constant, – plank constant, – optical energy band gap, – an exponent here it is 1/2 and – frequency of photon.

The estimated optical energy band gaps ( ) using an extrapolation of plot between and was depicted in Figure 4. It was observed from Figure 4 (b), (c), (d) that as time and calcination temperature rises optical energy band gap of $BaTiO_3$ nanoparticles also increases such as 2.9 eV, 3.1 eV, 3.8 eV, correspondingly. The comparative study of change in absorbance edge and bandgap was confirmed that as the calcination temperature and calcination time increases, absorbance edge goes to shift towards lower wavelength side, which is responsible to increase the band gap of $BaTiO_3$ nanoparticles.

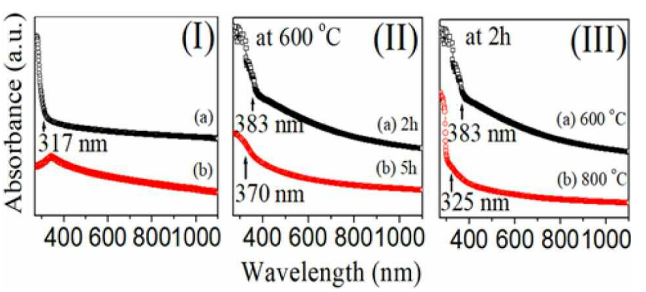

Figure 3. Optical absorbance spectra of $BaTiO_3$ nanoparticles (I) (a) calcinated at 100 °C for 1 hour and (b) commercially available, (II) calcinated at 600 °C for (a) 2 hours and (b) 5 hours and

(III) for 2 hours calcinated at (a) 600 °C and (b) 800 °C.

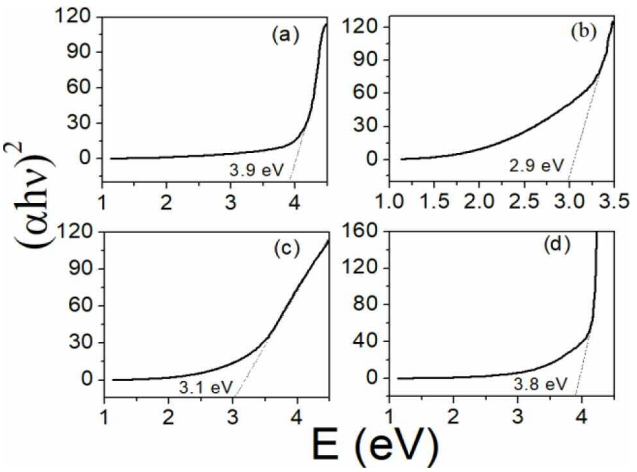

Figure 4. Optical band gap of BaTiO3 nanoparticles (a) commercially available, calcinated next to (b) 600 ℃, 2 hours, (c) 600 ℃, 5 hours, and (d) 800 ℃, 2 hours.

The Optical Band Structure and density of states

The optical spectra were intended with help of interband transition and explained its electronic structure. The Brillouin zone of $BaTiO_3$ nano particles was showed in Figure 6 along the high symmetry 3 directions. The density functional theory was used as coded in quantum ESPRESSO Software[8–9] to estimate energy bands. The band structure of cubic $BaTiO_3$nanoparticleswas estimated using ultrasoft and norm-conserving scalar relativistic type of hybrid pseudo potential functional with the PAW (projector augmented wave) method generated by AD Corso #3# generated by atomic #4# code in QE to approximate under GGA in ab initio electronic structure and EBS calculations. The structure of (a) $BaTiO_3$ amorphous and (b) crystalline $BaTiO_3$ nanoparticles was showed in Figure5.

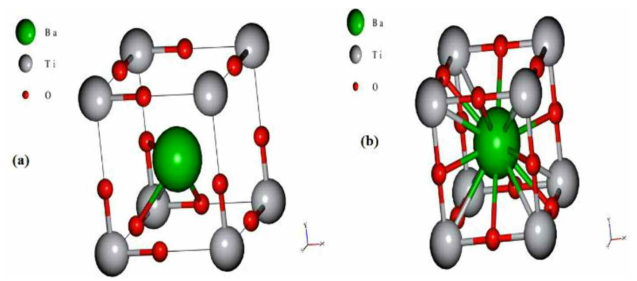

Figure 5. Structure of (a) amorphous $BaTiO_3$ and (b) crystalline $BaTiO_3$ nanoparticles.

It is a generality of pseudopotential, PAW, and allows for DFT designs to be accomplished through PBE[9]. The (MCB) minimum conduction band and (MVB) maximum valence band as label in Figure 6 displays indirect band, lowest band gap at and highest band gap at R points of Brillouin zone. Values of indirect band gap obtained from Figure 6 as 1.707 eV, 1.673 eV, 1.685 eV, and 1.673 eV of $BaTiO_3$ nanoparticles (a) commercially available, calcinated (b)

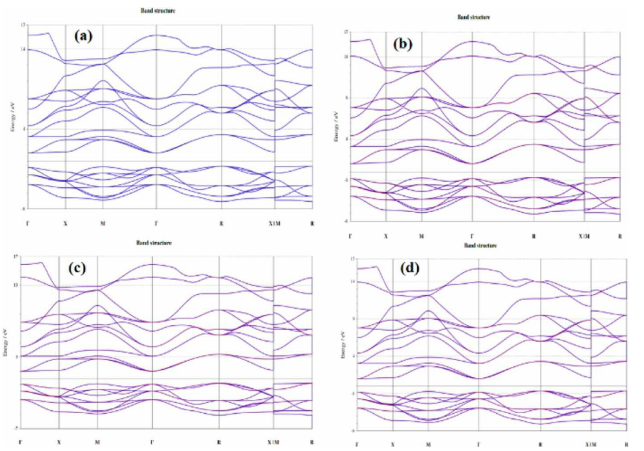

Figure 6. The Optical energy band structure of $BaTiO_3$ nanoparticles using PBE along with high symmetry way in Brillouin zone.

at 600 for 2 hours, (c) at 600 for 5 hours and, (d) at 800 for 2 hours, respectively. The values of energy of HOMO, LUMO and indirect band gap was tabulated in Table 1. The observed band gaps from DFT are somehow lower than graphically calculated band gap 2.9 eV, 3.1 eV, 3.8 eV, and 3.9 eV using UV–VIS data. Fermi level energy. The change in the band gaps obtained from DFT and UV–VIS data may occur due to the local-density approximation[10–11]. Figure 7 exhibits the optical energy band structure of $BaTiO_3$ nanoparticles where the optical energy (eV) at y axis contrasted with high symmetry way in Brillouin zone in x axis. This optical energy band structure was showed after the PBE functional pragmatic as exchange relationship. The straight line which is separated the valence band and conduction band at 0 eV is known asDensity of state using PBE exchange correlation versesenergy range from –37 eV to 17 eV was observed in Figure 7. The valance band region lies from –37 eV to –1.5 eV and conduction band region lies from 0.5 eV to 17 eV. No peak was observed between valance band and conduction band means there is no electronic state available at all[12–14].

Table 1. The values of Energy of HOMO, LUMO and Indirect Band Gap.

S. No.	Name	a=b=c	HOMO (eV)	LUMO (eV)	Indirect Band Gap (eV)
1	BTO	4.821	-1.0360	0.7496	1.7856
2	BTO (a)	4.0366	-0.6317	1.0753	1.707
3	BTO (b)	4.0242	-0.7665	0.9068	1.6733
4	BTO (c)	4.01754	-0.6658	1.0187	1.6845
5	BTO (d) commercial	4.036533	-0.5756	1.0978	1.6734

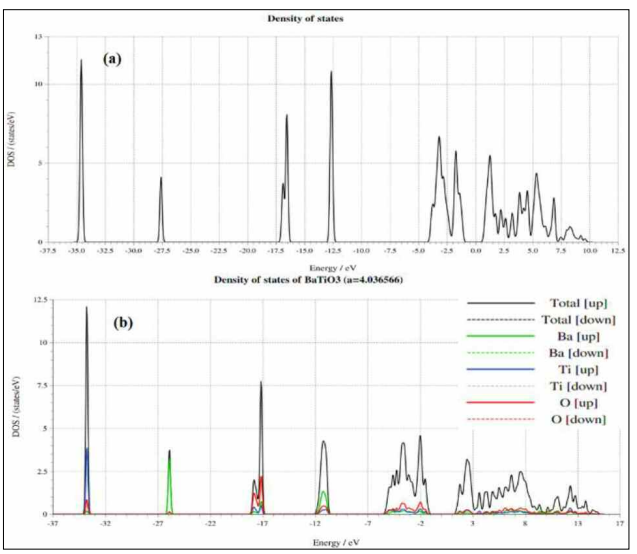

Figure 7. Density of state of BaTiO3 nanoparticles using PBE exchange correlation.

Dielectric Properties

The dielectric profile of synthesized BaTiO3 nanoparticles calcinated with varying temperature and time was investigated in the form of dielectric permittivity and dielectric loss with changing temperature and frequency.

The dielectric constant (ε) was obtained using this formula6.

$$\varepsilon' = \frac{Ct}{(\varepsilon_0 A)} \qquad (2)$$

where ε_0– permittivity of free space, ε' – dielectric constant of samples, t – thickness of pellet, C – capacitance of fabricated capacitor, and A – area of pellet.

The dielectric constant (ε') of BaTiO3 with changing temperature and frequency was depicted in Figure 8. The nominal feature was observed in Figure 8 that with increase in frequency, primarily ε' decreases quickly. As frequency exceeds than 1 kHz, ε' becomes constant for entirely $BaTiO_3$ nanoparticles. It was investigated from Figure 8 that even though (a) commercially available $BaTiO_3$ nanoparticles have maximum value of ε' but prepared BaTiO3 nanoparticles calcinated (b) at 600 ℃ for 2 hours also own advanced value than (c) at 600 ℃ for 5 hours and (d) at 800 ℃ for 2 hours. Moreover, ε' of all BaTiO3 nanoparticles displays dramatic nature with temperature range from 30 ℃ to 170 ℃ (Figure 8).

Ceramic materials exhibit electronic, ionic, and interfacial polarizations. In the lower frequency region, interfacial polarization is active whereas electronic and ionic polarizations are prevailed in the high frequency region. Therefore, as frequency increases from 1 MHz

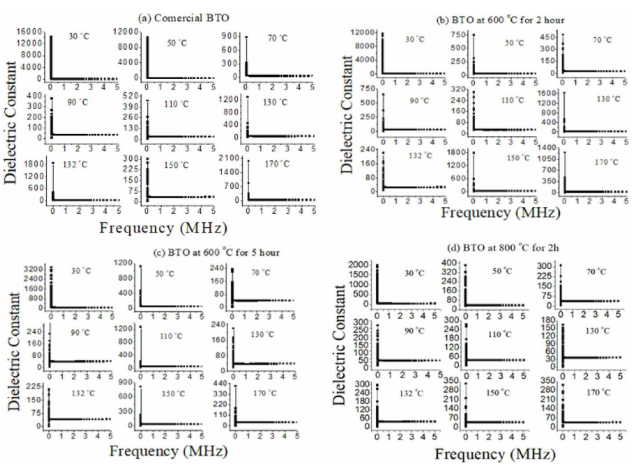

Figure 8. Dielectric constant with varying frequency and temperature of BaTiO3 nanoparticles.

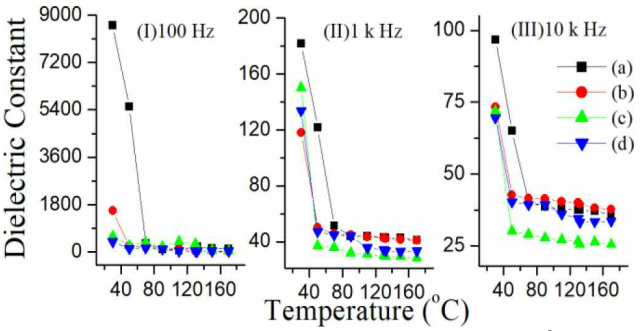

Figure 9. The Dielectric constant (ε') with temperature at (I) 100 Hz, (II) 1 kHz and (III) 10kHz of BaTiO3 nanoparticles (a)commercially available, calcinated at (b) 600 ℃, 2 hours (c) 600 ℃, 5 hours and (d) 800 ℃, 2 hours.

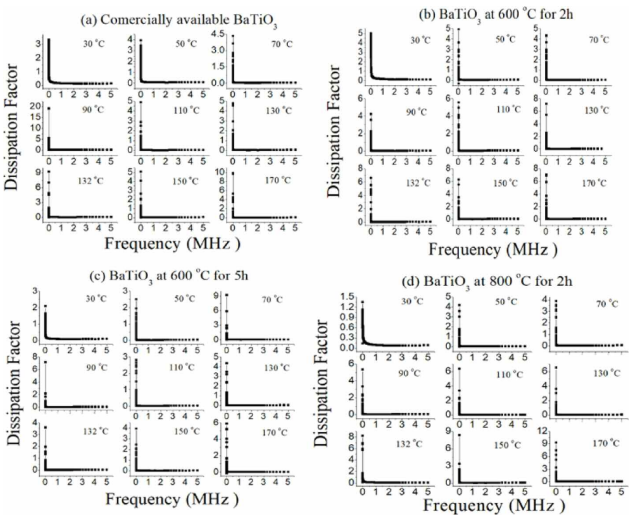

Figure 10. Dissipation factor with varying frequency and temperature (30–170) of BaTiO3 nanoparticles.

to 5 MHz, dipoles are totally immobile which decreases ε' approaching nearly constant value due to threatened interfacial polarization5.ε' with temperature at (I) 100 Hz, (II) 1 kHz and (III) 10 kHz was illustrated in Figure 9 for BaTiO3 nanoparticles (a) commercially available, (b) at 600 ℃ for 2 hours (c) at 600 ℃ for 5 hours and (d) at 800 ℃ for 2 hours. It was observed from Figure 9 that at initial temperature up to 70 ℃ at all frequencies (a) commercially existing BaTiO3 nanoparticles show extreme (ε') dielectric constant but on increasing temperature (b) The synthesized BaTiO3 nano particles which was calcinated at 600 ℃ for 2 hours becomes foremost than other samples at extreme frequency. This provides an outstanding relationship between optical energy band gap and dielectric properties. There are two noteworthy features were found from results: (i) ε' is increasing and optical energy gap reducing as particle size decreases in all BaTiO3 nanoparticles at high temperature and frequency. (ii) BaTiO3 nanoparticles which was calcinated at 800 ℃ for 2 hours is ultrapure than other synthesized BaTiO3. The dissipation factor of BaTiO3 nanoparticles with changing temperature and frequency was showed in Figure 10. Figure 10 (a–d) shows that dissipation factor primarily declines as frequency rises then befits almost constant (0.1–5 MHz). Furthermore, dissipation factor increases with rising temperature from 30 ℃ to 170 ℃. The dissipation factor was found to lower at 30 ℃ for all synthesized BaTiO3. BaTiO3 nanoparticles calcinated at 800 ℃ for 2 hours (Figure (10 d)) possess minimum dissipation factor owing to less impurity existing in BaTiO3 nanoparticles calcinated at 800 ℃, 2 hours.

Conclusion

BaTiO3 nanoparticles has been prepared by Sol-Gel route where samples were calcinated at 100 , 600 and 800 with varying time. The synthesized BaTiO3 nanoparticles which was calcinated at 800 for 2 hours found ultra-pure which confirmed using XRD. Band structure of BaTiO3nanoparticles using PBE along extreme symmetry direction in Brillouin zone was confirmed the formation of indirect band gap at and R.The values of indirect band gap obtained as 1.707 eV, 1.673 eV, 1.685 eV, and 1.673 eV of BaTiO3 nanoparticles commercially available, calcinated at 600 for 2 hours, for 5 hours and at 800 for 2 hours, respectively.There are two noteworthy features were obtained as of results: (i) ε' is cumulative and optical energy gap reducing as particle size decreases in all BaTiO3 nanoparticles at high temperature and frequency. (ii) BaTiO3 nanoparticles which was calcinated at 800 ℃ for 2 hours is ultrapure than other synthesized BaTiO3.

Acknowledgment

The authors are thankful for the funding agencies for SERB funded project no. EMR/2016/2156.

References

[1] M. Khan, M. Kumari, H. Pawar, U.K. Dwivedi, R.Kurchania,D. Rathore, Applied Physics A, 127(2021) 654–662.

[2] U.K. Dwivedi, M. Kumari, M. Khan, H. Pawar, R.Singhal,D. Rathore, Applied Physics A, 127 (2021)431–442.

[3] H. Pawar, M. Khan, C. Mitharwal, U.K. Dwivedi, S. Mitra, D. Rathore, Royal Society of Chemistry Advances. 10 (2020) 35265–35272.

[4] M. Khan, H. Pawar, M. Kumari, C. Patra, G. Patel, U.K. Dwivedi, D. Rathore, Journal of Alloys and Compounds. 840 (2020) 155596.

[5] H. Pawar, D. Kumar, U.K. Dwivedi, D. Rathore, Applied Innovative Research. 01 (2019) 75–77.

[6] M. Khan, H. Pawar, M. Kumari, D. Rathore, U.K. Dwivedi, Applied Innovative Research. 01 (2019) 93–95.

[7] H. Pawar, M. Khan, M. Kumari, T, Prasad, U.K. Dwivedi, D. Rathore, Applied Physics A, 127 (2021) 384–394.

[8] P. Giannozzi, S. Baroni, N. Bonini, M. Calandra, R. Car, C. Cavazzoni, D. Ceresoli, J. of phys: Cond. matter21 (2009) 395502.

[9] 9. P. Giannozzi, O. Andreussi, T. Brumme, O. Bunau, M. B. Nardelli, M. Calandra, R. Car, J. of Phys: Cond.Matter. 29 (2017) 465901.

[10] J. P. Perdew, K. Burke, M. Ernzerh, Phys. Rev. letters 77 (1996) 3865.

[11] S. Saha, T. P. Sinha, A. Mookerjee, Phy. Review B. 62 (2000) 8828.

[12] Razak, N. A. Abd, N. A. Zabidi, A. N. Rosli, AIP Conference Proceedings. 1875 (2017) 020017.

[13] Z.–X. Chen, Y. Chen, Y. S. Jiang, J. Phys. Chem. B. 105 (2001) 5766–5771.

[14] A. Ali, I. Khan, Z. Ali, F. Khan, I. Ahmmad.Int. J.l of Mod. Phy. B. 33 (2019) 1950231.